JHEP PROCEEDINGS

Corfu Summer Institute on Elementary Particle Physics, 1998

The MSSM neutral Higgs boson masses at the two-loop level

Wolfgang Hollik *

Institut für Theoretische Physik, Universität Karlsruhe, D-76128 Karlsruhe, Germany
E-mail: Wolfgang.Hollik@physik.uni-karlsruhe.de

ABSTRACT: Feynman-diagrammatic calculations are presented for the masses of the neutral $\mathcal{CP}$-even Higgs bosons in the Minimal Supersymmetric Standard Model (MSSM), complete at the one-loop level and including the two-loop leading QCD corrections. The results are valid for arbitrary values of the parameters of the MSSM and represent the currently most precise predictions within the Feynman-graph approach. The impact on the mass of the lightest Higgs boson is discussed and a comparison with the results obtained by the renormalization group method is performed.

1. Introduction

The search for the lightest Higgs boson provides a direct and very stringent test of SUSY. A precise prediction for the mass of the lightest Higgs boson in terms of the relevant SUSY parameters hence is crucial in order to determine the discovery and exclusion potential of LEP2 and the upgraded Tevatron and also for physics at the LHC, where a high-precision measurement of the mass of this particle might be possible.

In the MSSM the mass of the lightest Higgs boson, m_h, is restricted at the tree level to be smaller than the Z-boson mass. This bound, however, is strongly affected by the inclusion of radiative corrections. The dominant one-loop corrections arise from the top and scalar-top sector via terms of the form $G_F m_t^4 \ln(m_{\tilde{t}_1} m_{\tilde{t}_2}/m_t^2)$ [1]. They increase the predicted values of m_h and yield an upper bound of about 150 GeV. These results have been improved by performing a complete one-loop calculation in the on-shell scheme, which takes into account the contributions of all sectors of the MSSM [2, 3, 5]. Beyond one-loop order renormalization group (RG) methods have been applied in order to obtain leading logarithmic higher-order contributions [6, 7, 8, 9], and a diagrammatic calculation of the dominant two-loop contributions in the limiting case of vanishing $\tilde{t}$-mixing and infinitely large M_A and $\tan\beta$ has been carried out [10].

Recently a Feynman-diagrammatic calculation of the leading two-loop corrections of $\mathcal{O}(\alpha\alpha_s)$ to the masses of the neutral $\mathcal{CP}$-even Higgs bosons has been performed [11]. They have been combined with the complete one-loop diagrammatic calculation [12] to obtain in this way the currently most precise prediction for m_h within the Feynman-diagrammatic approach, for arbitrary values of the parameters of the Higgs and scalar top sector of the MSSM. Further refinements concerning the leading two-loop Yukawa corrections of $\mathcal{O}(G_F^2 m_t^6)$ [7, 15] and of leading QCD corrections beyond two-loop order are also included.

2. Outline of the calculation

The Higgs sector of the MSSM contains two doublets $H_i = \begin{pmatrix} H_i^2 \\ H_i^1 \end{pmatrix}$, with the components

$$H_1 = \begin{pmatrix} v_1 + (\phi_1^0 + i\chi_1^0)/\sqrt{2} \\ \phi_1^- \end{pmatrix},$$
$$H_2 = \begin{pmatrix} \phi_2^+ \\ v_2 + (\phi_2^0 + i\chi_2^0)/\sqrt{2} \end{pmatrix}. \qquad (2.1)$$

*work done in collaboration with Sven Heinemeyer and Georg Weiglein.

The tree level Higgs potential can be written as follows:

$$V = m_1^2 H_1^2 + m_2^2 H_2^2 + \epsilon_{ij}(m_{12}^2 H_1^i H_2^j + \text{h.c.}) + \frac{g^2+g'^2}{8}(H_1^2 - H_2^2)^2 + \frac{g^2}{4}(H_1 H_2)^2 . \tag{2.2}$$

Diagonalization of the mass matrices for the $\mathcal{CP}$-even and the $\mathcal{CP}$-odd scalars, following from the potential (2.2), leads to three physical particles: two $\mathcal{CP}$-even Higgs bosons H^0, h^0 and one $\mathcal{CP}$-odd Higgs boson A^0. The tree-level masses of h^0, H^0 follow from the coefficients $m_{\phi_1}^2, m_{\phi_2}^2$ and $m_{\phi_1\phi_2}^2$ of the quadratic terms of (2.2) in the $\phi_{1,2}$ basis. They are determined by the values of two input parameters, conventionally chosen as $\tan\beta = v_2/v_1$ and $M_A^2 = -m_{12}^2(\tan\beta + \cot\beta)$, where M_A is the mass of the $\mathcal{CP}$-odd A boson, and by the Z boson mass M_Z.

In the Feynman-diagrammatic approach the one-loop corrected Higgs masses are derived by finding the poles of the h, H-propagator matrix whose inverse is given by

$$\begin{pmatrix} q^2 - m_{H,\text{tree}}^2 + \hat{\Sigma}_H(q^2) & \hat{\Sigma}_{hH}(q^2) \\ \hat{\Sigma}_{hH}(q^2) & q^2 - m_{h,\text{tree}}^2 + \hat{\Sigma}_h(q^2) \end{pmatrix}, \tag{2.3}$$

where the $\hat{\Sigma}$ denote the full one-loop contributions to the renormalized Higgs-boson self-energies, i.e. including the counterterms. For these self-energies we take the result of the complete one-loop on-shell calculation of [3]. The agreement with the result obtained in [2] is better than 1 GeV for almost the whole MSSM parameter space.

As mentioned above the dominant contribution arises from the $t, \tilde{t}$-sector. The current eigenstates of the scalar quarks, $\tilde{q}_L$ and $\tilde{q}_R$, mix to give the mass eigenstates $\tilde{q}_1$ and $\tilde{q}_2$. The non-diagonal entry in the scalar quark mass matrix is proportional to the mass of the quark and reads for the $\tilde{t}$-mass matrix

$$m_t M_t^{LR} = m_t(A_t - \mu\cot\beta), \tag{2.4}$$

where we have adopted the conventions used in [4]. Due to the large value of m_t mixing effects have to be taken into account. Diagonalizing the $\tilde{t}$-mass matrix one obtains the eigenvalues $m_{\tilde{t}_1}$ and $m_{\tilde{t}_2}$ and the $\tilde{t}$ mixing angle $\theta_{\tilde{t}}$.

At one-loop, the dominant contributions proportional to $G_F m_t^4$ can be obtained by evaluating the contribution of the $t, \tilde{t}$-sector to the $\phi_{1,2}$ self-energies at zero external momentum from the Yukawa part of the theory (neglecting the gauge couplings). Accordingly, the one-loop corrected Higgs masses are derived by diagonalizing the mass matrix, given in the ϕ_1, ϕ_2 basis as

$$M_{\text{H}}^2 = \begin{pmatrix} m_{\phi_1}^2 - \hat{\Sigma}_{\phi_1}(0) & m_{\phi_1\phi_2}^2 - \hat{\Sigma}_{\phi_1\phi_2}(0) \\ m_{\phi_1\phi_2}^2 - \hat{\Sigma}_{\phi_1\phi_2}(0) & m_{\phi_2}^2 - \hat{\Sigma}_{\phi_2}(0) \end{pmatrix}. \tag{2.5}$$

Therein, the $\hat{\Sigma}$ are restricted to the Yukawa contributions of the $t, \tilde{t}$-sector to the renormalized one-loop $\phi_{1,2}$ self-energies. In this approximation one obtains the compact expressions

$$\begin{aligned} M_{H,h}^2 = {} & \frac{M_A^2 + M_Z^2 + \epsilon_t + \sigma_t}{2} \\ & \pm \Bigg[\frac{(M_A^2 + M_Z^2)^2 + (\epsilon_t - \sigma_t)^2}{4} \\ & - M_A^2 M_Z^2 \cos^2 2\beta \\ & + \frac{(\epsilon_t - \sigma_t)\cos 2\beta}{2}(M_A^2 - M_Z^2) \\ & - \lambda_t \sin 2\beta (M_A^2 + M_Z^2) + \lambda_t^2 \Bigg]^{1/2} \end{aligned} \tag{2.6}$$

with

$$\begin{aligned} \epsilon_t = {} & \frac{N_C G_F m_t^4}{\sqrt{2}\pi^2 \sin^2\beta} \Bigg[\log\left(\frac{m_{\tilde{t}_1} m_{\tilde{t}_2}}{m_t^2}\right) \\ & + \frac{A_t(A_t - \mu\cot\beta)}{m_{\tilde{t}_1}^2 - m_{\tilde{t}_2}^2} \log\frac{m_{\tilde{t}_1}^2}{m_{\tilde{t}_2}^2} \\ & + \frac{A_t^2 (A_t - \mu\cot\beta)^2}{(m_{\tilde{t}_1}^2 - m_{\tilde{t}_2}^2)^2} \times \\ & \times \left(1 - \frac{m_{\tilde{t}_1}^2 + m_{\tilde{t}_2}^2}{m_{\tilde{t}_1}^2 - m_{\tilde{t}_2}^2} \log\frac{m_{\tilde{t}_1}}{m_{\tilde{t}_2}}\right) \Bigg], \end{aligned}$$

$$\begin{aligned} \lambda_t = {} & \frac{N_C G_F m_t^4}{2\sqrt{2}\pi^2 \sin^2\beta} \Bigg[\frac{\mu(A_t - \mu\cot\beta)}{m_{\tilde{t}_1}^2 - m_{\tilde{t}_2}^2} \log\frac{m_{\tilde{t}_1}^2}{m_{\tilde{t}_2}^2} \\ & + \frac{2\mu A_t (A_t - \mu\cot\beta)^2}{(m_{\tilde{t}_1}^2 - m_{\tilde{t}_2}^2)^2} \times \\ & \times \left(1 - \frac{m_{\tilde{t}_1}^2 + m_{\tilde{t}_2}^2}{m_{\tilde{t}_1}^2 - m_{\tilde{t}_2}^2} \log\frac{m_{\tilde{t}_1}}{m_{\tilde{t}_2}}\right) \Bigg], \end{aligned}$$

$$\begin{aligned} \sigma_t = {} & \frac{N_C G_F m_t^4}{\sqrt{2}\pi^2 \sin^2\beta} \frac{\mu^2 (A_t - \mu\cot\beta)^2}{(m_{\tilde{t}_1}^2 - m_{\tilde{t}_2}^2)^2} \times \\ & \times \left[1 - \frac{m_{\tilde{t}_1}^2 + m_{\tilde{t}_2}^2}{m_{\tilde{t}_1}^2 - m_{\tilde{t}_2}^2} \log\frac{m_{\tilde{t}_1}}{m_{\tilde{t}_2}}\right] . \end{aligned} \tag{2.7}$$

These formulae contain the masses $m_{\tilde{t}_{1,2}}$ of the top squarks, the Higgs mass parameter μ of the superpotential, and the non-diagonal entry A_t in the stop mass matrix. By comparison with the full one-loop result [3] it has been shown that these contributions indeed contain the bulk of the one-loop corrections. Typical differences to the full one-loop result are of the order of 5 GeV.

The leading two-loop corrections have been obtained in [11] by calculating the $\mathcal{O}(\alpha\alpha_s)$ contribution of the $t,\tilde{t}$-sector to the renormalized Higgs-boson self-energies at zero external momentum from the Yukawa part of the theory. At the two-loop level the matrix (2.3) consists of the renormalized Higgs-boson self-energies

$$\hat{\Sigma}_s(q^2) = \hat{\Sigma}_s^{(1)}(q^2) + \hat{\Sigma}_s^{(2)}(0), \quad s = h, H, hH, \tag{2.8}$$

where the momentum dependence is neglected only in the two-loop contribution. The Higgs-boson masses at the two-loop level are obtained by determining the poles of the matrix $\Delta_{\rm Higgs}$ in Eq. (2.3).

The renormalization is performed in the on-shell scheme. The counterterms in the Higgs sector are derived from the Higgs potential (2.2), analogously to the 1-loop calculation. The renormalization conditions for the tadpole counterterms are chosen in such a way that they cancel the tadpole contributions in one- and two-loop order. On-shell mass renormalization is imposed for the A^0 boson. The renormalization in the t-$\tilde{t}$-sector is performed in the same way as in [4]. The one-loop counterterms δm_t, $\delta m_{\tilde{t}_1}$, $\delta m_{\tilde{t}_2}$ for the top-quark and top-squark masses and $\delta\theta_{\tilde{t}}$ for the mixing angle contribute, which enter via the subloop renormalization. The appearance of the $\tilde{t}$-mixing angle $\theta_{\tilde{t}}$ reflects the fact that the current eigenstates, $\tilde{t}_L$ and $\tilde{t}_R$, mix to give the mass eigenstates $\tilde{t}_1$ and $\tilde{t}_2$. Since the non-diagonal entry in the scalar quark mass matrix is proportional to the quark mass the mixing is particularly important in the case of the third generation scalar quarks. The mixing angle counterterm $\delta\theta_{\tilde{t}}$ is chosen in such a way that there is no transition between $\tilde{t}_1$ and $\tilde{t}_2$ when $\tilde{t}_1$ is on-shell. The numerical result, however, is insensitive to the choice of the renormalization point. Counterterms for μ and $\tan\beta$ do not appear in $\mathcal{O}(\alpha_s)$.

The results are analytical expressions for the two-loop self-energies in terms of the SUSY parameters $\tan\beta$, M_A, μ, $m_{\tilde{t}_1}$, $m_{\tilde{t}_2}$, $\theta_{\tilde{t}}$, and the gluino mass $m_{\tilde{g}}$, to be inserted together with the one-loop self-energies into the propagator matrix (2.3).

Two further steps of refinement have been implemented into the prediction for m_h, which are shown separately in the plots below. The leading two-loop Yukawa correction of $\mathcal{O}(G_F^2 m_t^6)$ is taken over from the result obtained by renormalization group methods [7, 15]. The second step of refinement concerns leading QCD corrections beyond two-loop order, taken into account by using the $\overline{MS}$ top mass, $\overline{m}_t = \overline{m}_t(m_t) \approx 166.5$ GeV, for the two-loop contributions instead of the pole mass, $m_t = 175$ GeV. In the $\tilde{t}$ mass matrix, however, we continue to use the pole mass as an input parameter. Only when performing the comparison with the RG results we use $\overline{m}_t$ in the $\tilde{t}$ mass matrix for the two-loop result, since in the RG results the running masses appear everywhere. This three-loop effect gives rise to a shift up to 1.5 GeV in the prediction for m_h.

The complete one-loop calculation together with the leading two-loop corrections and the other corrections beyond $\mathcal{O}(\alpha\alpha_s)$ have been implemented into the `FORTRAN` code *FeynHiggs* [13]. This code can be linked to existing programs as a subroutine, thus providing an accurate calculation of m_h and m_H, which can be used for further phenomenological analyses. For a detailed study of the MSSM Higgs masses see [14].

3. Discussion

For the numerical evaluation we have chosen two values for $\tan\beta$ which are favored by SUSY-GUT scenarios [16]: $\tan\beta = 1.6$ for the $SU(5)$ scenario and $\tan\beta = 40$ for the $SO(10)$ scenario. Other parameters are $M_Z = 91.187$ GeV, $M_W = 80.375$ GeV, $G_F = 1.16639\,10^{-5}$ GeV^{-2}, $\alpha_s(m_t) = 0.1095$, and $m_t = 175$ GeV. For the figures below we have furthermore chosen $M = 400$ GeV (M is the soft SUSY breaking parameter in the chargino and neutralino sector), $M_A = 500$ GeV, and $m_{\tilde{g}} = 500$ GeV as typical values (if not indicated differently). The scalar top masses and

the mixing angle are derived from the parameters $M_{\tilde{t}_L}$, $M_{\tilde{t}_R}$ and M_t^{LR} of the $\tilde{t}$ mass matrix (our conventions are the same as in [4]). In the figures below we have chosen $m_{\tilde{q}} \equiv M_{\tilde{t}_L} = M_{\tilde{t}_R}$.

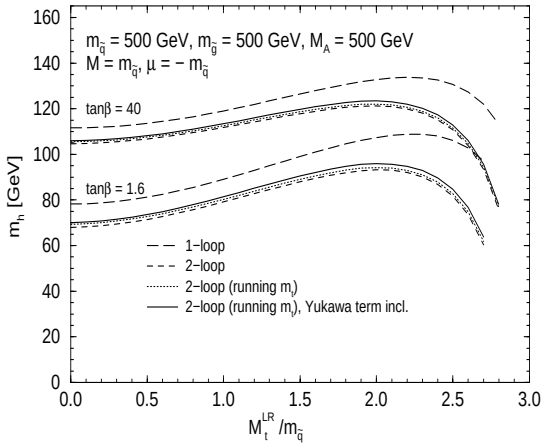

Figure 1: One- and two-loop results for m_h as a function of $M_t^{LR}/m_{\tilde{q}}$ for two values of $\tan\beta$.

The plot in Fig. 1 shows the result for m_h obtained from the diagrammatic calculation of the full one-loop and leading two-loop contributions. The two steps of refinement discussed above are shown in separate curves. For comparison the pure one-loop result is also given. The results are plotted as a function of $M_t^{LR}/m_{\tilde{q}}$, where $m_{\tilde{q}}$ is fixed to 500 GeV. The qualitative behavior is the same as in [11], where the result containing only the leading one-loop contribution (and without further refinements) was shown. The two-loop contributions give rise to a large reduction of the one-loop result of 10–20 GeV. The two steps of refinement both increase m_h by up to 2 GeV. A minimum occurs for $M_t^{LR} = 0$ GeV which we refer to as 'no mixing' (different from section 1). A maximum in the two-loop result for m_h is reached for about $M_t^{LR}/m_{\tilde{q}} \approx 2$ in the $\tan\beta = 1.6$ scenario as well as in the $\tan\beta = 40$ scenario. This case we refer to as 'maximal mixing' (differently from section 1). The maximum is shifted compared to its one-loop value of about $M_t^{LR}/m_{\tilde{q}} \approx 2.4$. The two steps of refinement have only a negligible effect on the location of the maximum.

We now turn to the comparison of our diagrammatic results with the predictions obtained

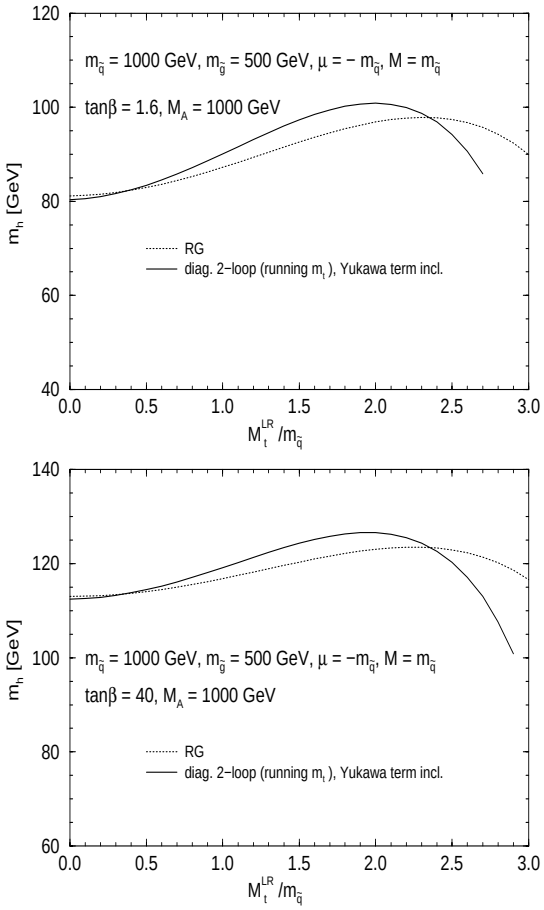

Figure 2: Comparison between the Feynman-diagrammatic calculations and the results obtained by renormalization group methods [8]. The mass of the lightest Higgs boson is shown for the two scenarios with $\tan\beta = 1.6$ and $\tan\beta = 40$ for increasing mixing in the $\tilde{t}$-sector and $m_{\tilde{q}} = M_A$.

via renormalization group methods. We begin with the case of vanishing mixing in the $\tilde{t}$ sector and large values of M_A, for which the RG approach is most easily applicable and is expected to work most accurately. In order to study different contributions separately, we have first compared the diagrammatic one-loop on-shell result [3] with the one-loop leading log result (without renormalization group improvement) given in [9] and found very good agreement, typically within 1 GeV. We then performed a leading log expansion of our diagrammatic result (which corresponds to the two-loop contribution in the RG approach) and also found agreement with the full

two-loop result within about 1 GeV. Finally, we have compared our diagrammatic result for the no-mixing case including the refinement terms with the RG results [1] obtained in [8]. After the inclusion of the refinement terms the diagrammatic result for the no-mixing case agrees very well with the RG result. The deviation between the results exceeds 2 GeV only for $\tan\beta = 1.6$ and $m_{\tilde{q}} < 150$ GeV. For smaller values of M_A the comparison for the no-mixing case looks qualitatively the same. For $\tan\beta = 1.6$ and values of M_A below 100 GeV slightly larger deviations are possible. Since the RG results do not contain the gluino mass as a parameter, varying $m_{\tilde{g}}$ gives rise to an extra deviation, which in the no-mixing case does not exceed 1 GeV. Varying the other parameters μ and M in general does not lead to a sizable effect in the comparison with the corresponding RG results.

We now consider the situation when mixing in the $\tilde{t}$ sector is taken into account. We have again compared the full one-loop result with the one-loop leading log result used within the RG approach [9] and found good agreement. Only for values of M_A below 100 GeV and large mixing deviations of about 5 GeV occur. In Fig. 2 our diagrammatic result including the refinement terms is compared with the RG results [8] as a function of $M_t^{LR}/m_{\tilde{q}}$ for $\tan\beta = 1.6$ and $\tan\beta = 40$. For larger $\tilde{t}$-mixing sizable deviations between the diagrammatic and the RG results occur, which can exceed 5 GeV for moderate mixing and become very large for large values of $M_t^{LR}/m_{\tilde{q}}$. As already stressed above, the maximal value for m_h in the diagrammatic approach is reached for $M_t^{LR}/m_{\tilde{q}} \approx 2$, whereas the RG results have a maximum at $M_t^{LR}/m_{\tilde{q}} \approx 2.4$, i.e. at the one-loop value. Varying the value of $m_{\tilde{g}}$ in our result leads to a larger effect than in the no-mixing case and shifts the diagrammatic result relative to the RG result within ± 2 GeV.

So far, the results of our diagrammatic on-shell calculation and the RG methods have been compared in terms of the parameters $M_{\tilde{t}_L}$, $M_{\tilde{t}_R}$ and M_t^{LR} of the $\tilde{t}$ mixing matrix, since the available numerical codes for the RG results [8, 9] are given in terms of these parameters. However, since the two approaches rely on different renormalization schemes, the meaning of these (non-observable) parameters is not precisely the same in the two approaches starting from two-loop order. Indeed we have checked that assuming fixed values for the physical parameters $m_{\tilde{t}_1}$, $m_{\tilde{t}_2}$, and $\theta_{\tilde{t}}$ and deriving the corresponding values of the parameters $M_{\tilde{t}_L}$, $M_{\tilde{t}_R}$ and M_t^{LR} in the on-shell scheme as well as in the $\overline{MS}$ scheme, sizable differences occur between the values of the mixing

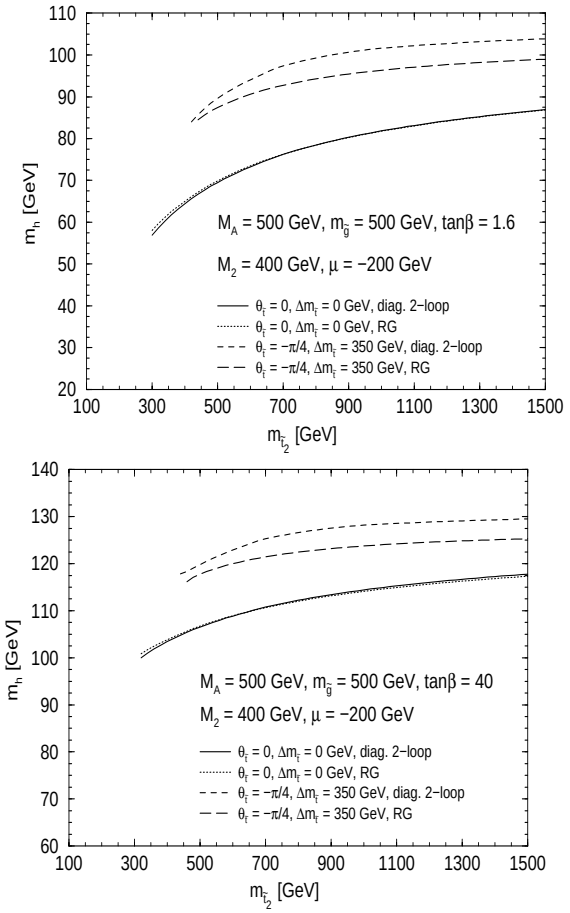

Figure 3: Comparison between the Feynman-diagrammatic calculations and the results obtained by renormalization group methods [8]. The mass of the lightest Higgs boson is shown for the two scenarios with $\tan\beta = 1.6$ and $\tan\beta = 40$ as a function of the heavier physical $\tilde{t}$ mass $m_{\tilde{t}_2}$. For the curves with $\theta_{\tilde{t}} = 0$ a mass difference $\Delta m_{\tilde{t}} = 0$ GeV is assumed whereas for $\theta_{\tilde{t}} = -\pi/4$ we chose $\Delta m_{\tilde{t}} = 350$ GeV, for which the maximal Higgs masses are achieved.

[1] The RG results of [8] and [9] agree within about 2 GeV with each other.

parameter M_t^{LR} in the two schemes, while the parameters $M_{\tilde{t}_L}$, $M_{\tilde{t}_R}$ are approximately equal in the two schemes. Thus, part of the different shape of the curves in Fig. 2 may be attributed to a different meaning of the parameter M_t^{LR} in the on-shell scheme and in the RG calculation.

For the purpose of comparing results obtained in different renormalization schemes it is very desirable to express the prediction for the Higgs-boson masses in terms of physical observables, i.e. the physical masses and mixing angles of the model instead of unphysical parameters. As a step into this direction we compare in Fig. 3 the diagrammatic results and the RG results as a function of the physical mass $m_{\tilde{t}_2}$ and with the mass difference $\Delta m_{\tilde{t}} = m_{\tilde{t}_2} - m_{\tilde{t}_1}$ and the mixing angle $\theta_{\tilde{t}}$ as parameters. In the context of the RG approach the running $\tilde{t}$ masses, derived from the $\tilde{t}$ mass matrix, are considered as an approximation for the physical masses. The range of the $\tilde{t}$ masses appearing in Fig. 3 has been constrained by requiring that the contribution of the third generation of scalar quarks to the ρ-parameter [4] does not exceed the value of $1.3 \cdot 10^{-3}$. As in the comparison performed above, in Fig. 3 very good agreement is found between the results of the two approaches in the case of vanishing $\tilde{t}$ mixing. For the maximal mixing angle $\theta_{\tilde{t}} = -\pi/4$, however, the diagrammatic result yields values for m_h which are higher by about 5 GeV.

References

[1] H. Haber, R. Hempfling, *Phys. Rev. Lett.* **66**, 1815 (1991);
Y. Okada, M. Yamaguchi, T. Yanagida, *Prog. Theor. Phys.* **85**, 1 (1991);
J. Ellis, G. Ridolfi, F. Zwirner, *Phys. Lett.* B **257**, 83 (1991); *Phys. Lett.* B **262**, 477 (1991);
R. Barbieri, M. Frigeni, *Phys. Lett.* B **258**, 395 (1991)

[2] P. Chankowski, S. Pokorski, J. Rosiek, *Nucl. Phys.* B **423**, 437 (1994)

[3] A. Dabelstein, *Nucl. Phys.* B **456**, 25 (1995); *Z. Phys.* C **67**, 495 (1995)

[4] A. Djouadi, P. Gambino, S. Heinemeyer, W. Hollik, C. Jünger, G. Weiglein, *Phys. Rev. Lett.* **78**, 3626 (1997); *Phys. Rev.* D **57**, 4179 (1998)

[5] J. Bagger, K. Matchev, D. Pierce, R. Zhang, *Nucl. Phys.* B **491**, 3 (1997)

[6] J. Casas, J. Espinosa, M. Quirós, A. Riotto, *Nucl. Phys.* B **436**, 3 (1995), E: *ibid.* B **439**, 466 (1995)

[7] M. Carena, J. Espinosa, M. Quirós, C. Wagner, *Phys. Lett.* B **355**, 209 (1995)

[8] M. Carena, M. Quirós, C. Wagner, *Nucl. Phys.* B **461**, 407 (1996)

[9] H. Haber, R. Hempfling, A. Hoang, *Z. Phys.* C **75**, 539 (1997)

[10] R. Hempfling, A. Hoang, *Phys. Lett.* B **331**, 99 (1994)

[11] S. Heinemeyer, W. Hollik, G. Weiglein, *Phys. Rev.* D **58**, 091701 (1998)

[12] S. Heinemeyer, W. Hollik, G. Weiglein, *Phys. Lett.* B **440**, 296 (1998)

[13] S. Heinemeyer, W. Hollik and G. Weiglein, hep-ph/9812320. *FeynHiggs* is available via its WWW page
`http://www-itp.physik.uni-karlsruhe.de/feynhiggs`.

[14] S. Heinemeyer, W. Hollik, G. Weiglein, hep-ph/9812472 (*Eur. Phys. J.* C, to appear)

[15] M. Carena, P. Chankowski, S. Pokorski, C. Wagner, FERMILAB-PUB-98/146-T, hep-ph/9805349.

[16] M. Carena, S. Pokorski, C. Wagner, *Nucl. Phys.* B **406**, 59 (1993);
W. de Boer et al., *Z. Phys.* C **71**, 415 (1996)